PDR

Per Stewart Schneider

89319-01

==========

MANUSCRIPT FOR PUBLICATION

==========

Draft: 16 Nov 89

Acute Lesions in Skin Produced by ^{235}Uranium-Carbide Microspheres

P. Donald Forbes[1], William C. Roesch[2] and S.Z. Mikhail[3]

[1]Biohazard Control Office
Temple University
3307 North Broad Street
Philadelphia, PA 19140

[2]1646 Butternut
Richland, WA 99352

[3]Deceased
(Formerly U.S. Naval Radiological Defense Laboratory
San Francisco, CA 94140)

	==========	
	NB: This draft does not	
	include revised references,	
	citations or acknowledge-	
	ments.	
	Rads-->Gy not fixed.	
	Appendix?	
	==========	

DF03
0/1

270087

OEM-8 reports general

X M-13 Uranium

ABSTRACT

Tissue effects were evaluated after activated uranium microspheres were applied to the skin of mice and swine. Radiation doses absorbed in tissue were estimated utilizing a beta extrapolation chamber and the beta "Transmission, Degradation and Dissipation" (TDD) model developed at the Naval Radiological Defense Laboratory. At a point on the circumference of a 4 mm radius circle, 100μ below the tissue surface, the doses ranged from 4×10^{0} to 3.5×10^{2} Gy as a function of particle size and exposure time. Ulcers in pig skin began at the site of contact and eventually became 0.5 - 8 mm in diameter. The post-irradiation syndrome also included pigmentation changes, inhibition of hair grown, desquamation, and contraction. The threshold dose from ulceration was not directly determined because a response was found at all doses used.

Similar changes were seen in particle-exposed mouse skin, but at significantly lower estimated doses. The inhibition of hair growth was used to calculate a dose-response curve for mouse skin. Although the study was originally designed to address a problem related to nuclear rocket reactor fuel, the findings provide some data relevant to the broader question of biological response to "hot particle" exposure.

Introduction

The operation of nuclear reactors encompasses a broad spectrum of health and safety concerns. One subset of management problems relates to near-microscopic radioactive debris referred to as "hot particles" or "fuel fleas". Identifying, containing and eliminating the particles is a physical problem; assessing the health aspect is a radiobiologic problem, currently hampered by incomplete knowledge about the consequences of extremely non-homogeneous distribution of radiation dose to target tissue such as skin.

Nearly three decades ago an analogous problem was recognized during the test firing of nuclear rocket reactor motors in the Nevada desert. Exhaust gasses carried neutron-activated microspheres from the reactor core's uranium fuel, posing a contamination risk to the test site and its surrounds. A laboratory simulation was undertaken to determine the most likely biologic response following skin contact with such debris.[1] A series of dosimetric models had been developed to handle the radiometric data and to help interpret the findings for the benefit of the test site management.

We report here the results of the laboratory study which involved application of reactor-activated rocket fuel beads to the skin of miniature pigs, primarily so that the biologic data will be available for further analysis.

We offer this laboratory study as an extension of a field evaluation and not as a simulation of the contemporary power reactor hot particle problem; the particle content, shape and emission characteristics vary considerably, and dosimetric approaches have evolved rapidly.[2] The appendix provides a bridge to contemporary analyses.

Materials and Experimental Procedure

Each of the sources used in this study was a pyrolytic graphite-coated microsphere of 93% enriched 235-uranium carbide (UC_2). The smaller sources ranged in diameter from 138 to 154 microns (μ), the larger ones from 277μ to 328μ, including the graphite coating. Unexposed fuel beads from the same batch were used to determine the thickness of the graphite coating. The coating was split and removed by applying pressure on a particle placed between two glass slides. The coating thickness was determined to be between 23μ and 27μ. Thus, for the whole set of UC_2 microspheres used, the approximate core diameter ranged from 113μ to 303μ. All diameters shown subsequently include the graphite coating.

The microspheres were examined, measured and photographed at 400x magnification. The intact sources appeared to be almost perfectly spherical. In some instances removal of the graphite layer for determination of the coating thickness revealed a little roughness on the UC_2 surface.

Activation was accomplished in the pneumatic tube facility of a pool-type research reactor at the Industrial Reactor Laboratory, Plainsboro, New Jersey. The nominal flux of the 5 megawatt IRL reactor was 10^{13} neutr $cm^{02}sec^{-1}$.

Animal Experiments

Nineteen microspheres were activated and placed on two pigs (Fig. 4). Twenty microspheres were used to irradiate skin on 38 haired mice (Fig. 4, 6, 7) and 10 rhino mice (Fig. 9).

Following reactor activation the individual microspheres were sandwiched between thin films of polyethylene (density: 1.2 mg cm^{-2}), and these packets were taped to the shaved skin of the experimental animals for various periods of time ranging from 5 minutes to 3 hours. In each case, the microsphere was separated from the skin by the 10-micron thick film. The microspheres were spaced at laterial distances adequate to insure separate treatment areas.

The miniature swine (Hanford-Labco Cross variety; Battelle-Northwest Laboratory) were sparsely haired[3] and they had a variable amount of dark-colored skin. The pigs weighted approximately 20 kg at the time of exposure. The area selected for study extended from the hip to the shoulder and from the mid-dorsum to a point 30 cm down each side. Haired mice ($C_{57}BL/10J$) were treated by applying the hot particle to plucked skin during the resting (telogen) phase of the skin cycle.

The rhino mice[4] had no surface hair. The treated sites on both mice and swine were permanently identified with tattoo grid marks; nevertheless, the unique syndrome of changes that accompanied even the smallest ulcers provided positive identification of radiation-induced lesions.

Daily observations were made on the animals during the first month after exposure, and then the detailed examinations were continued twice weekly for 16 weeks. Lesions were measured with a ruler and recorded to the nearest half-millimeter (those less than 1 mm are shown as 0.5 mm). Tissue biopsies from some of the exposed area were examined histologically using a variety of staining techniques[5].

To Appendix ?

Determination of the Number of Equivalent Fissions

Calculation of the number of fissions occuring in each particle during activation through knowledge of the neutron flux, the fission cross-section the amount of fissionable material in the particle, and the exact length of activation period was tried but found unsatisfactory. An undue amount of care was required in experimental determination of the integrated thermal, epithermal, and fast neutron flux and in calculating the correction factors due to the shadowing effect particles had on each other. This technique was, therefore, abandoned in favor of direct estimation of the number of fissions in each individual particle by measurement of its total decay gamma radiation in a high pressure ionization chamber. The chamber used was identical to an instrument designed and built at Oak Ridge National laboratory and described by Jones and Overman[6]. A partial description of the ion chamber was given by Miller[7] along with computed energy calibration curves based on the response of the instrument to a number of radionuclides of known disintegration rate and energy level decay scheme. Using the computed calibration curves and the decay schemes of individual fission products, Miller predicted the response of the instrument to decay gamma from fission product mixtures.

Using Miller's computations, Mackin et al.[8] constructed a response curve of current per fission versus time after fission, which they verified experimentally. Their experience with the chamber showed that measurements on representative samples generally agreed within ±10% of radiochemically determined values of number of fissions.

Instrumental precision was further tested in the following manner[9]. The number of fissions in each of six particles was determined with this chamber and checked by quantitative chemical analysis and gamma counting at Los Alamos Scientific Laboratory. Table 1 presents the data obtained. The percentage difference between the corresponding values of the number of fissions did not exceed 7% (column 7).

Table I

COMPARISON OF FISSION DATA

Particle Number	Particle Diameter	Number of Equivalent Fissions			Difference	Difference % of Average
		NRDL	LASL	Average		
1	285	5.9×10^{12}	5.73×10^{12}	5.84×10^{12}	0.23×10^{12}	3.95
2	312	7.69×10^{12}	7.45×10^{12}	7.57×10^{12}	0.24×10^{12}	3.17
3	295	6.59×10^{12}	6.38×10^{12}	6.48×10^{12}	0.21×10^{12}	3.24
4	152	6.53×10^{11}	6.19×10^{11}	6.36×10^{11}	0.34×10^{11}	5.35
5	149	6.15×10^{11}	5.74×10^{11}	5.94×10^{11}	0.41×10^{11}	6.91
6	147	5.60×10^{11}	5.33×10^{11}	5.44×10^{11}	0.23×10^{11}	4.23

Particles used for animal exposure were transported immediately to NRDL for determination of the number of fissions and beta dose rate. Each particle was placed in a clear thin-walled plastic tube and measured in a 4-pi chamber at least twice within a period of 2 to 5 days following its arrival. Its beta dose rate was determined by the method described below.

Beta Dose-Rate Measurements and Calculations the Extrapolation Chamber

Dose-rate measurements for each particle were made using an extrapolation chamber of the type described by Loevinger[10]. The measurements made were of the ionization within a volume of air of uniform thickness between two tissue equivalent electrodes. The electrode area (5.07 cm^2), and the distance

between the electrodes defined the ionization volume[11], Fig. 2.

The electrodes were made of a mylar film stretched tautly over a brass embroidery loop. A circular area, 11.3 cm^2, of each absorber was sprayed with a thin coat of graphite to give an electrically conducting lower surface.

On the top surface of the absorber a strip of graphite was painted leading from the metal hoop to two pinholes at the edge of the lower graphited area. This established electrical conductivity between the brass hoop and the graphited area on the lower side of the absorber. A fine wire in contact with the metal hoop was connected to the input of the vibrating reed electrometer.

The coordinates of the center of the collecting electrode were established using a pointer mounted on a modified microscope stage. This device enabled the experimenter to center the particle with respect to the collecting electrode and ensured reproducible geometry.

The extrapolation chamber measurements were validated by comparison between the dose-rates obtained at NRDL and those obtained at Oak Ridge National Laboratory using an independently constructed extrapolation chamber. Good agreement between the data was assumed to indicate that the apparatus was free of important systematic errors. Before each series of measurements the apparatus was checked for consistency using a standard beta source.

Beta dose criteria and models are described in the Appendix.

equivalent to the diameter of the denuded, oozing sore, and in turn, the diameter of the eschar which subsequently filled the denuded space.

The development of the lesion was more rapid at the sites of higher absorbed doses; in contrast, healing events appeared more rapidly after lower doses. Moist desquamation appeared at the sites of particle contact as early as the second day after exposure. The area of involvement gradually spread outward to its maximum size; the time required for full development was approximately two weeks for the smaller particles, and up to four weeks for the larger particles. Dry eschar formation commenced within three days after the appearance of an ulcer; by six weeks after exposure, all lesions were dry. Scarification was completed in most cases by twelve weeks. Residual evidence of damage included scars, flaking (radiodermatitis), depilation, and in appropriate areas, pigment alterations. Reappearance of inflammatory changes was noted at irregular intervals, although healing proceeded with less complexity than that reported in much larger lesions[15].

RESULTS AND DISCUSSION

Observations on Swine

The site of each exposure was erythematous by the time the particles were removed from the skin. No effort was made to quantify the intensity of the change, but the extent of visible reddening was most intense and extensive by 24 hours, and it diminished during the next few days. Thereafter, erythema reappeared irregularly.

Hairs continued to grow in the previously shaved skin surrounding treated areas, but all hair growth ceased in the skin displaying early erythema. By 30 days after exposure, some growth was evident again in the affected areas, and only the radiation scars were permanently epilated.

Darkening of normally pigmented skin formed a halo around the center of the exposed spot, beginning on the third day. The most intense darkening occurred before the end of the third week (Fig. 3), and fading began thereafter. A narrow, irregular ring of hyperpigmentation remained permanently around the edge of the scar. The skin nearest the particle became involved in desquamation, followed by protracted healing. This area was permanently depigmented (Fig. 3).

The disappearance of early erythema coincided with the appearance of one or more very small vesicles at the exposure site. These gave way to the formation of a single bulla which was always transient, usually granular in appearance, and somewhat variable in contour. With the loss of this surface material, each lesion then developed into an oozing sore indicating loss of functional epidermis. Cavitation of larger lesions provided evidence of loss of some dermis as well. The depth of damage would be expected to bear a direct relationship with the diameter of the lesion, and the appearance of the ulcers indicated that this was the case. A direct measurement of depth of lesions was not feasible, and quantitative data were based exclusively on surface dimensions.

None of the lesions was biopsied during the formation of the ulcer. Because cell and tissue events can only be inferred from clinical appearance, the extent of histologic destruction, as well as the precise mode of repair could not be determined. Consequently, the choice of a term to designate the lesions is an arbitrary one. The simplifying assumption was made that large and small lesions were qualitatively similar. Therefore, the word "ulcer" was chosen to designate one endpoint. As used here, "ulcer" diameter is

TABLE II
Dosimetry Data and Responses (Pig Skin)

Particle Number	Particle Diameter (μ)	Exposure (hr:min)	Point Depth Dose 100μ in tissue (Rads)	Kraus' Dose (Rads)	Ulcer Diameter (mm)	Depigmentation Diameter (mm)
1	304	1:00	2.32×10^6	1.11×10^4	5	10
2	(fractured)	-	-	-	-	-
3	292	1:52	3.55×10^6	1.51×10^4	6	14
4	295	1:00	2.35×10^6	1.09×10^4	5	12
5	296	2:00	7.40×10^6	3.52×10^4	8	17
6	328	1:40	3.85×10^6	1.98×10^4	7	20
7	294	2:03	3.80×10^6	1.73×10^4	6	14
8	305	0:41	1.53×10^6	7.32×10^3	5	12
9	283	0:30	1.23×10^6	5.40×10^3	4	8
10	308	0:30	1.51×10^6	7.49×10^3	5	10
11	149	3:05	1.70×10^6	2.89×10^6	4	8
12	150	3:00	1.37×10^6	2.31×10^3	3	9
13	148	0:30	2.40×10^5	4.05×10^2	0.5	1
14	140	0:30	2.86×10^5	4.44×10^2	0.5	2.5
15	152	1:30	6.42×10^5	1.06×10^3	2	5
16	148	1:00	5.69×10^5	9.44×10^2	0.5	3
17	153	1:28	5.14×10^5	7.71×10^2	2	5
18	145	1:00	4.52×10^5	7.70×10^2	1	5
19	154	1:45	7.38×10^5	1.21×10^3	2	6
20	144	1:28	5.63×10^5	9.21×10^2	0.5	5

TABLE III
DOSIMETRY DATA AND RESPONSES (MOUSE)

Mouse Number	Particle Diameter (μ)	Exposure (Minutes)	Point Depth Dose 100μ in tissue (Rads)	Krebs' Dose (Rads)	Hair Growth Delay Diameter (mm)
1	141	25	1.04×10^5	1.55×10^2	5
2	286	17	2.82×10^5	1.19×10^3	(biopsied)
3	293	18	2.82×10^5	1.23×10^3	7
4	146	24	1.20×10^5	1.88×10^2	5.5
5	304	25	5.46×10^5	2.49×10^3	7
6	293	12	1.67×10^5	7.23×10^2	8
7	146	14	6.00×10^4	9.27×10^1	3.5
8	304	14	2.60×10^5	1.18×10^3	9
9	141	13	4.66×10^4	6.78×10^1	4.5
10	287	07	1.08×10^5	4.53×10^2	5
11	148	13	5.79×10^4	9.12×10^1	3.5
12	288	13	1.53×10^5	6.50×10^2	5
13	286	13	1.91×10^5	8.03×10^2	(biopsied)
14	146	28	1.05×10^5	1.59×10^2	3.5
15	304	28	4.51×10^5	2.02×10^3	9
16	293	29	3.51×10^5	1.51×10^3	(biopsied)
17	141	29	9.60×10^4	1.30×10^2	5
18	148	27	1.05×10^5	1.64×10^2	4.5
19	288	15	5.35×10^4	8.69×10^1	7
20	286	28	3.60×10^5	1.49×10^3	(biopsied)
21	277	08	1.01×10^5	4.37×10^2	5
22	154	08	3.66×10^4	6.17×10^1	3.5
23	287	25	3.44×10^5	1.44×10^3	7
24	142	04	1.31×10^4	1.31×10^4	3.5
25					(died)
26	287	05	6.12×10^4	2.54×10^2	5.5
27	141	14	4.75×10^4	6.86×10^1	3.5
28	293	15	2.24×10^5	9.68×10^2	5
29	151	15	5.35×10^4	8.69×10^1	3.5
30	154	17	7.19×10^4	1.20×10^2	2
31	[illegible]	16	2.03×10^5	8.01×10^2	7
32	142	20	6.08×10^4	8.83×10^1	(biopsied)
33	318	20	2.78×10^5	1.31×10^3	7
34	150	23	6.52×10^5	1.03×10^2	4.5
35	138	12	2.49×10^4	3.43×10^1	1.5
36	138	23	5.66×10^4	7.51×10^1	1.5
37	304	22	3.07×10^5	1.38×10^3	9
38	141	22	6.69×10^4	9.50×10^1	8
39	318	24	1.75×10^5	8.20×10^2	(biopsied)
40	142	14	3.85×10^4	5.51×10^1	2
41	151	12	3.70×10^4	5.87×10^1	5.5
42					(died)
43	277	13	1.51×10^5	5.92×10^2	5
44	154	12	4.66×10^4	7.68×10^1	2
45	138	12	2.32×10^4	3.17×10^1	2
46	293	12	1.54×10^5	6.80×10^2	4

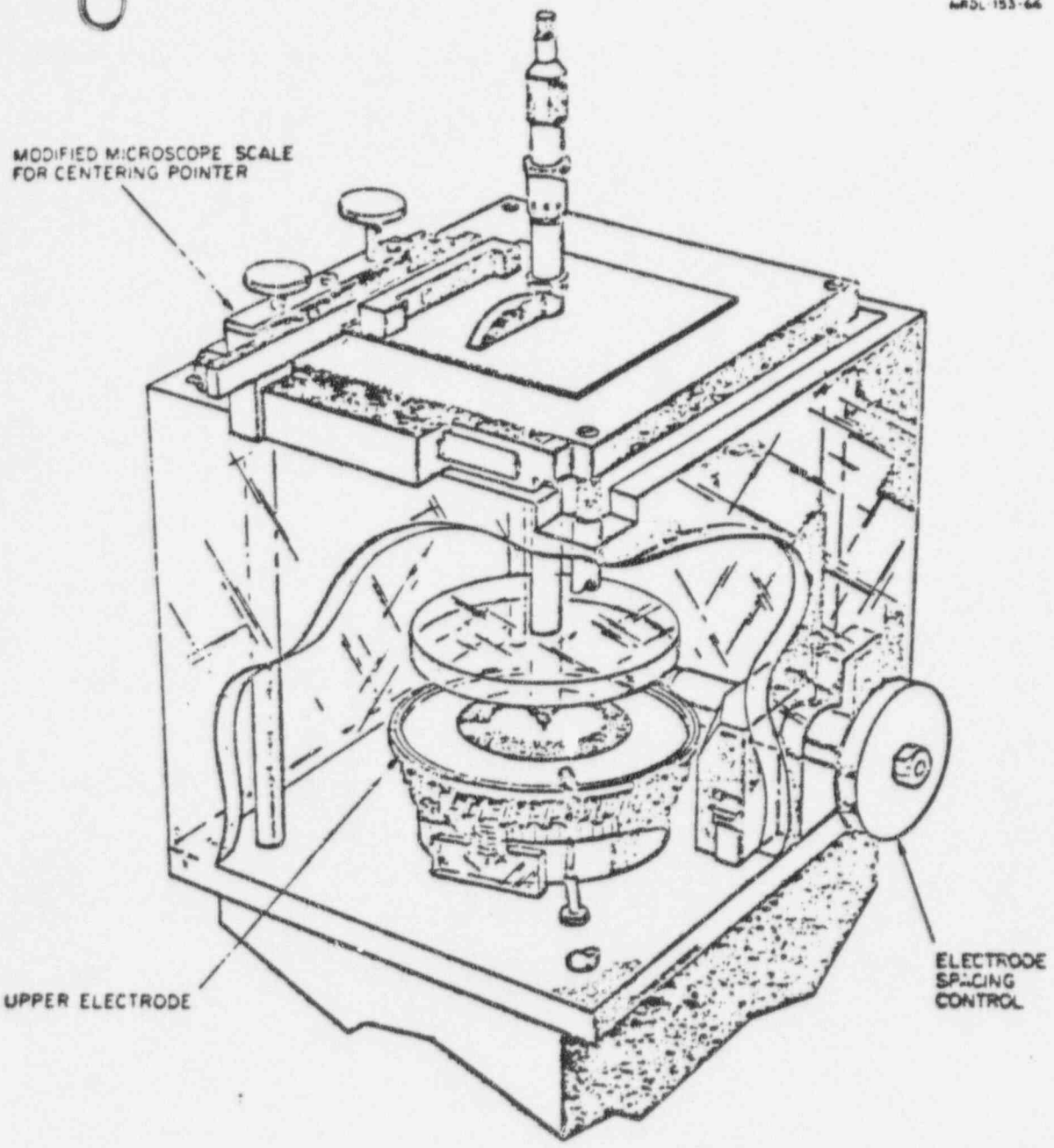

Figure 1. Schematic Diagram of the Extrapolation Chamber. (From Reference 12)

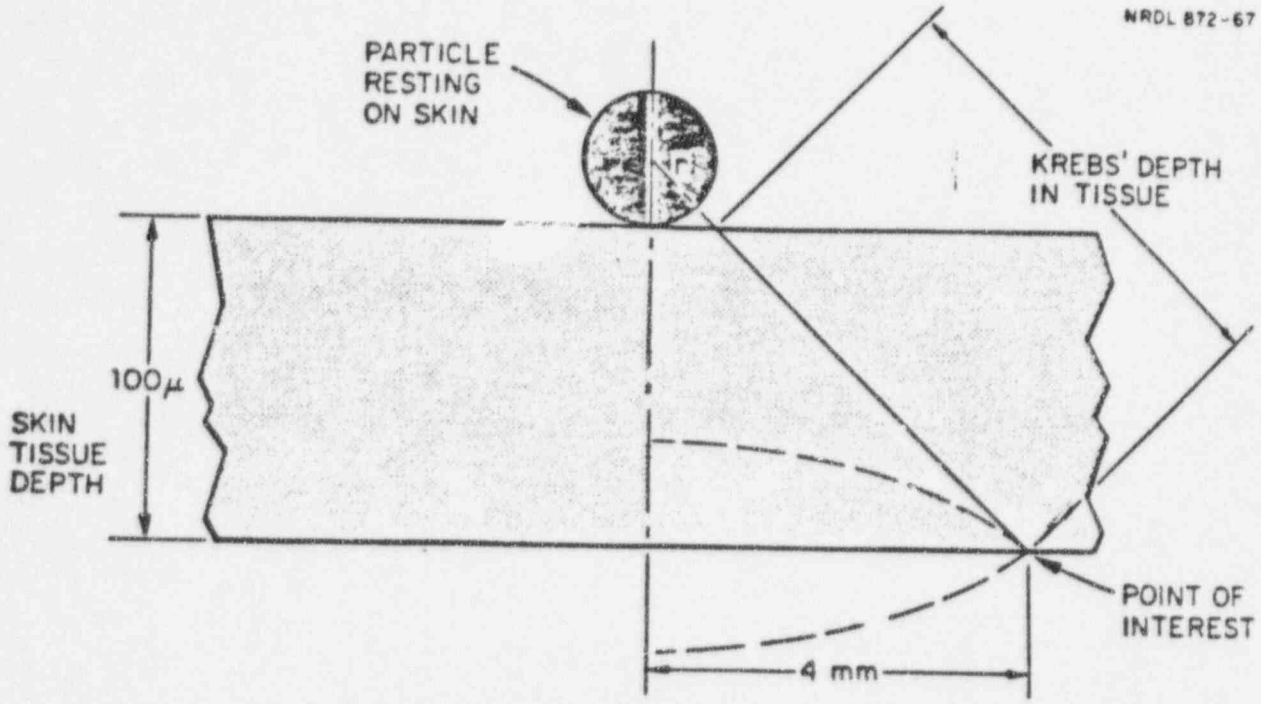

$$\text{KREBS' DEPTH} = \frac{100}{100+r}\sqrt{(100+r)^2+(4000)^2}\,\mu$$

Figure 2: Diagram of Krebs' Concept (not to scale).
From Reference 12.
See also Figure 10.

Figure 4. Hot particle-induced lesions in pig skin. Frames numbered left to right & top to bottom.

Frame 1.	Photographic technique for recording changes in lesions. Fixed-distance close-up camera assures identical format for each frame.
Frame 2 through 7.	Particle exposure #19 (Krebs' dose 1.20×10^3 rads). Photographs taken on the following days post-exposure: 13, 21, 24, 26, 45, 66. Magnification: 1.4x.
Frames 8 through 15.	Particle exposure #11 (Krebs' dose 2.88×10^3 rads). Days post exposure: 0, 13, 17, 21, 26, 29, 41, 66.
Frames 16 through 25.	Particle exposure #5 (Krebs' dose 3.51×10^4 rads). Days post-exposure: 0, 7, 9, 13, 19, 21, 26, 29, 36, 61.
Frame 26.	Particle exposure #13 (Krebs' dose 4.05×10^2 rads). Photograph was taken on day 49.
Frame 27.	Particle exposure #3 (Krebs' dose 1.50×10^4 rads). Photograph was taken on day 49 (see also Fig. 8 and histologic description in text).

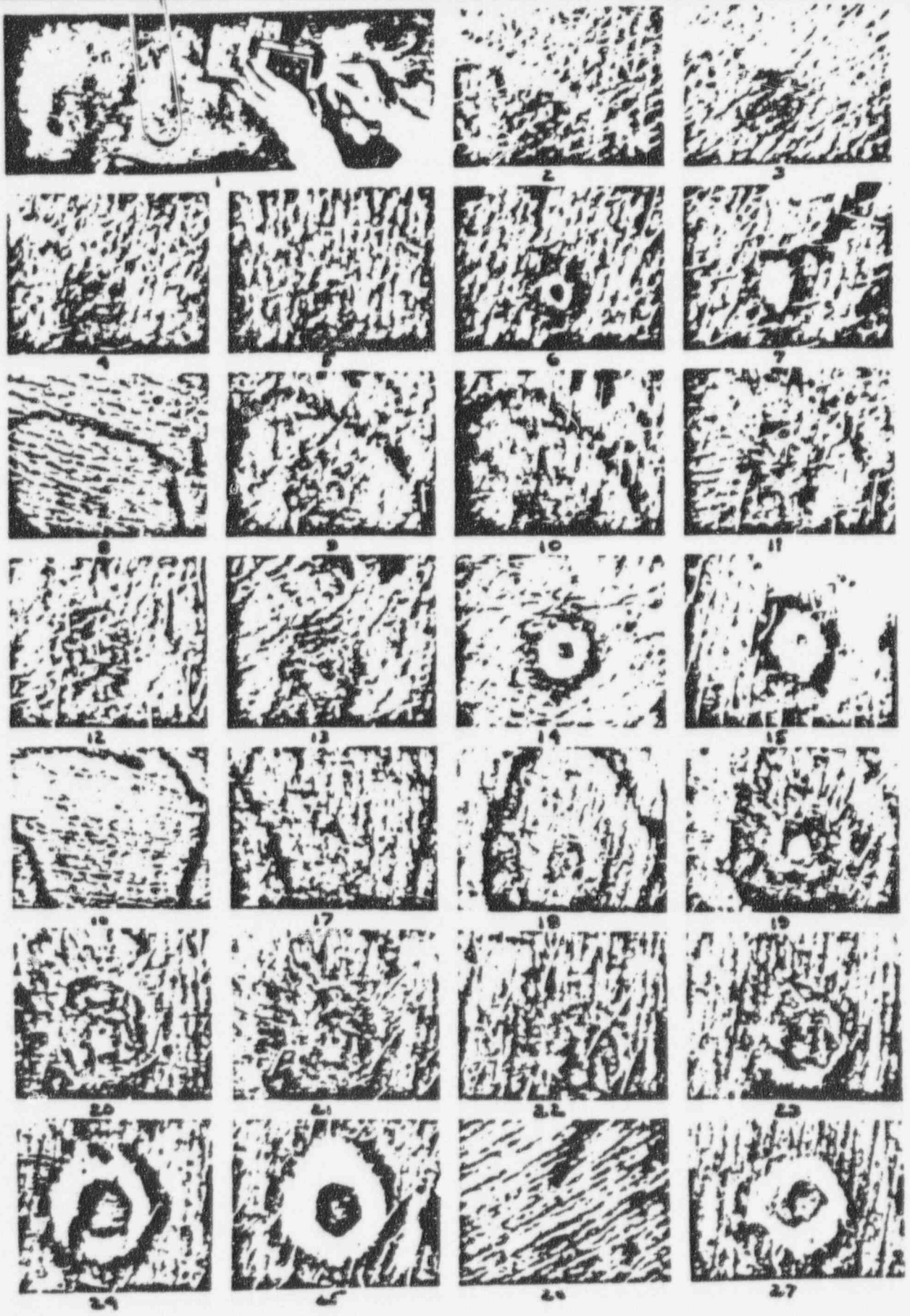

Fig. 3

Dose response curves for diameters of ulcer formation (UF) and depigmentation (DP) are shown in Fig. 4. These endpoints are strongly correlated with dose, and, not surprisingly, with each other (for UF vs. DP, r = 0.95).

Two excision biopsy specimens were removed from pigs. The first (Sport #3) had received 15 x 10^3 rads (Krebs') 55 days previously. A photograph of the skin surface is contained in Fig. 3, and the histologic appearance is shown in Fig. 8. Histologically, the lesion had sharply defined borders on the laterial edges, but it merged gradually into the connective tissue below. Tongues of epithelium from the surrounding epidermis could be seen growing in under the eschar. The regenerating epithelium was vascularized and hypertrophic with a rather thick stratum corneum. The epidermis immediately adjacent to the eschar and its overlying stratum corneum was amelanotic, although a few scattered DOPA-positive cells were present. Hypertrophy and bizarre mitotic figures were present. Abnormal amounts of melanin were contained in cells surrounding the vascular elements of the superficial dermis. Further from the eschar, there was an abrupt transition from hypopigmented to hyperpigmented epidermis and stratum corneum; some pigmented cells were present in the dermis. The epidermis of the hyperpigmented area was only slightly hypertrophic.

Site #13 was also biopsied at 55 days post-treatment. The Krebs' dose was 405 rads, and the ulcer had not exceeded 0.3 mm diameter. As was characteristic with the smaller lesions, healing was well underway. However, the lesion was qualitatively similar to the one described above, confirming the clinical impression that the radiation burns presented a continuum down to the smallest ulcers produced.

Observations on Mice

Qualitatively, most of the changes occurring in exposed mouse skin were similar to those seen in pig skin. However, comparable changes were elicited by much lower doses in mice, probably as a function of their thinner epidermis (Fig. 9). Inhibition of hair growth in mice is produced by relatively small doses of radiation (Fig. 5). The location and extent of damage was readily identified in the black-haired mice (Fig. 6, 7). Rhino mice have a life

expectancy of approximately 10-12 months[4]. Eleven months after the exposure of a group of 10 rhino mice, the lone survivor developed a tumor (a hemangioma) at the site of particle contact. The estimated Krebs' dose was 190 rads, and in the acute phase, an ulcer of less than 0.5 mm had developed.

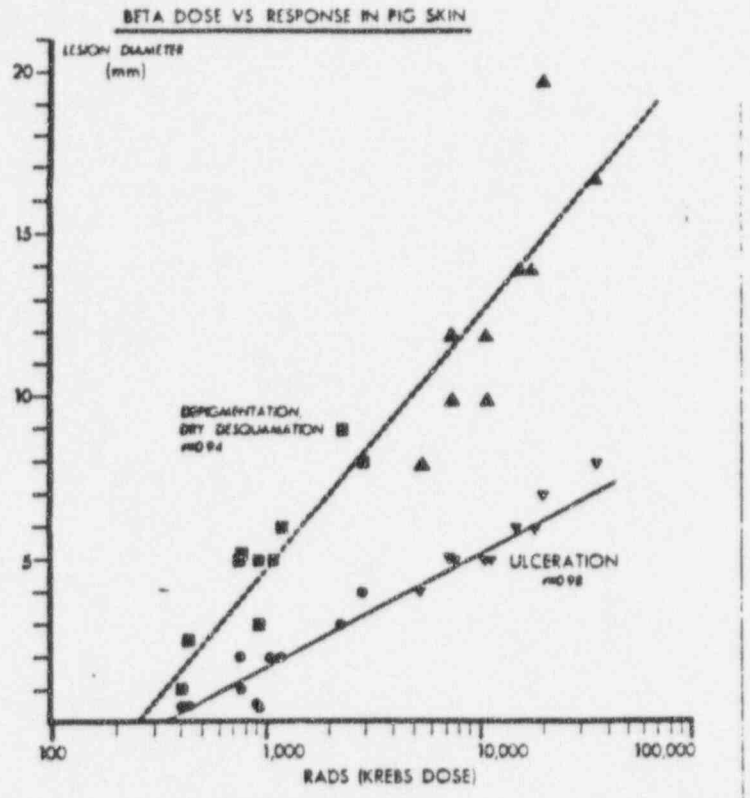

Figure 4. Small particles are represented by squares and circles. Large particles are represented by triangles. Curves fitted by least squares analysis (Ref. 16).

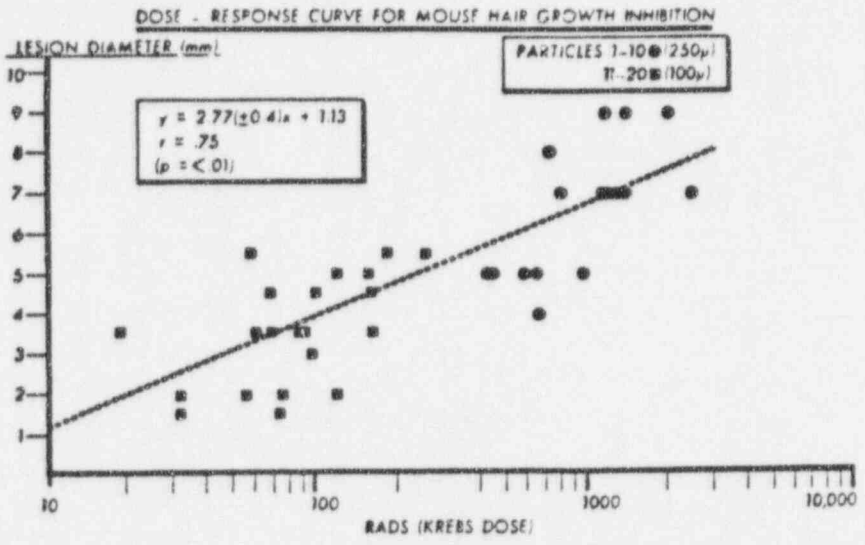

Figure 5. Large particles represented by circles, small particles represented by squares.

Discussion

In evaluating specific radiation hazards, it has sometimes been difficult to extrapolate from available data. For example, the degree of damage which could be expected from cosmic ray heavy nuclei posed a problem apparently not answerable from data on large-field radiation exposures. Consequently, Chase and Straile[17] and later Curtis et al.[18] developed methods for exposing skin and other tissues to collimated microbeams of x rays. In terms of equivalent absorbed doses, the response of tissue in such limited areas proved to be qualitatively different from that of tissue under conventional techniques.

The evaluation of radioactive microspheres ("hot particles") as a potential source of external radiation poses an analogous problem. Existing data on large field studies, sieve and grid exposures, and microbeams are probably insufficient for estimating acute responses and are almost certainly inadequate for the predicting of such late effects as carcinogenesis from hot particles. Relative to the size of the system being exposed, the hot particle may be represented reasonably well as a point source. Even if the emission from such a source were monochromatic, the absorbed doses at various distances would present a rather complex array of isodose curves influenced by distance and various absorber densities. The dosimetry problem is further complicated if the particle contains a mixture of isotopes.

Absorbed radiation is presented here as the "point-depth dose" 100 μ below the particle and as the "Krebs'dose". The distances involved are illustrated in Fig. 10 in proportion to one particle 300 μ in diameter and another particle 86μ in diameter. The "sensitive" layer of skin is represented schematically by the bar of tissue 100 μ thick since germinative cells and blood vessels supplying the epidermis of human and pig skin are, on the average, at that depth. Tissue absorption and distance account for the very significant difference between the point-depth and Krebs' doses from the same particle. The ratio of one dose to the other is a function of the particle size as well as the composite spectrum which is, in turn, dependent on the exposure time and duration. Although the Krebs'dose provides a better visual image of dose fall-off with distance, the two methods correlated about equally

well with the biologic responses recorded during this project (Table IV). However, under the conditions of these experiments, the two methods could not be exhaustively compared. Krebs' criterion, which carries with it the idea of area damage vs. a dose to a small volume around a point, has the apparent advantage of correcting for the effect of particle size (and thus the comparative path lengths in air and tissue) on absorbed dose (Fig. 10). For this reason, a fairer test of the Krebs' model would involve an experiment in which the full range of doses would be delivered by both large and small particles. At present, we have available for analysis only high doses delivered by large particles, and lower doses by small particles.

TABLE IV

CORRELATION COEFFICIENTS (r)

	Mouse Hair Growth Inhibition	Pig Skin	
		Ulcer	Depigmentation, Desquamation
Krebs' Dose	0.75	0.98	0.94
Point Depth Dose	0.74	0.96	0.94

Ionizing radiations, including beta particles, have induced cancer in skin[19-22]. Although there had not yet emerged a clear basis for evaluating the skin cancer risk of a specified hot particle incident, Krebs' provisional description of a potentially hazardous exposure was employees[11]; the production of a radiation-ulcer was emphasized mainly because it was felt that "cancer of the skin is consistently associated with the development of serious, non-healing or recurring, acute lesions of the skin"[12]. In turn, the preoccupation of this report with Krebs' doses and radiation ulcers is a result of an attempt to produce data on ulcer dose "thresholds" comparable to those cited above[12].

A variety of designations have been used in referring to skin lesions produced by radiation. Krebs[12] choose to use the categories employed primarily by

British workers: I (Erythema), II (Dry Desquamation), III (Moist Desquamation), IV (Ulceration). Other sources qualify category IV as severe ulceration, and add a fifth category (V Necrosis). Category V is considered to involve infection and other impediments to healing[23].

The bleeding lesion shown in frame 20 of Fig. 3 would fit Category IV (Ulceration, as described in References 12 and 23). The lesion shown in Frame 26 had passed through a stage characterized by moist desquamation (Category III). Qualitatively, it was similar to the larger lesions, but on the basis of its size, it is doubtful whether such a lesion would generally be called a severe ulcer. It is probable that for particle-induced lesions, Category IV ceases to exist somewhere between these extremes in size, and this possibility should be explored experimentally.

A model describing the radiation response for epidermal cell populations in mouse skin influenced the predictions of dose-response following particle exposure[12]. Further evidence for the validity of the mouse model has been presented by Energy et al.[24], although Archambeau and Mathieu[17] have given evidence from work in swine that available radiation-response models for skin are not entirely satisfactory. Coupled with the complexities in dosimetry models for point sources, these facts appear to underline the uncertainties that necessarily exist in interpreting and predicting particle-induced skin lesions.

Figure 6. $C_{57}BL$ mouse plucked (during telogen phase of hair cylce) and exposed 9 days before picture was taken. Krebs' dose 1.44×10^3 rads. Central eschar is surrounded by area of retarded hair growth.

Figure 7. Twelve days post-exposure, Krebs' dose 1.17×10^3 rads. Darker surrounding area indicates further hair growth in unaffected skin.

Figure 8. Photomicrograph of pig skin at site of exposure #3. Eschar appears on right, edge of ulcer at center, and peripheral skin is at left of photograph. See more detailed description in text. (H&E stain; scale shows one millimeter).

Figure 9. Rhino mouse, 7 days following a Krebs' dose of 1.78×10^3 rads.

7
9
6
8

Because all the skin exposures from these experiments resulted in ulcers as defined previously and with further experiments on uranium particles precluded by the closing of NRDL, the threshold dose for acute response was not determined. The data derived up to that time could be interpreted to indicate that 1) the minimum dose required to produce a small but recognizable ulcer is below 405 rads (Krebs) and 2) assuming a continued straight-line relationship, the UF and the DP approach zero at about 350 rads and 250 rads respectively (Fig. 4). However, it has not been determined from available data whether deviations exist at the origin end of the curve and so the extrapolation must be interpreted with caution.

Figure 10. Diagram showing relationships implied by the Krebs' concept.

A. Krebs' concept drawn to scale. The average epidermal thickness is represented by the dashed lines. Solid lines are drawn from the centers of two particles to a point 4 mm lateral and 100 microns deep. That portion of the solid line within the "epidermis" is termed the Krebs' depth, and it is significantly influenced by particle size.

B. Schematic representation of swine epidermis, drawn to the same scale as above. Epidermal ridges and cones, enclosing the vascularized dermal papillae, produce the irregular wavy line which characterizes the undersurface of the epidermis. In addition, naturally-occurring creases in the skin distort the entire epidermis into a series of hills and valleys.

C. Krebs' concept superimposed on diagram of swine epidermis. The local configuration of the skin, as well as the location of the particle, can influence absorbed dose at any significant distance.

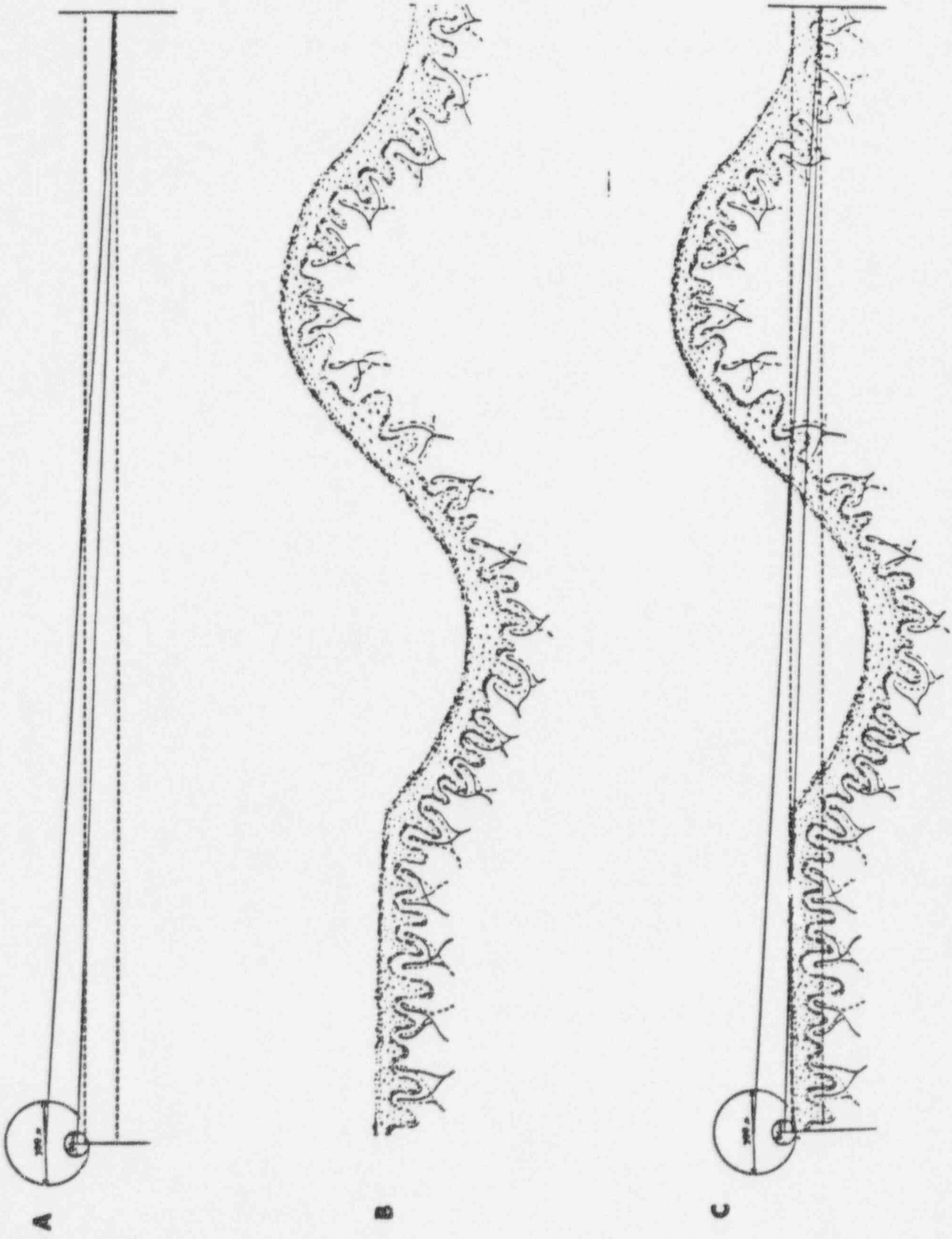

29

Fig. 10

References

Charles, M. W. 1976. A Study of Carcinogenic Risks Following The Non Uniform Irradiation of Skin. I: An Appraisal of Theoretical Models (Report RD/B/N3484 Central Electricity Generating Board Research Dept. Berkeley Nuclear Laboratories). II: A Proposal For an Animal Experiment (Report RD /B/N3633 Central Electricity Generating Board Research Dept. Berkeley Nuclear Laboratories).

1. Forbes, P.D. 1969. Effects of single microscans... Rad. Res. 39 (1465th Dec-8).

~~2. Forbes, P. D. 1977. II. Strontium Silicate Microspheres. In preparation.~~

3. Forbes, P. D. 1967. Radiation Effects in Swine. I. Vascular Supply of the Skin and Hair. U.S. Naval Radiological Defense Laboratory, USNRDL-TR-67-141.

4. Forbes, P. D. 1965. Experimentally-Induced Neoplasma in the Skin of Mice. I. Single-Dose Effects of DMBA in Haired, Hairless, and Rhino Mice. J. Invest. Dermatol. 44:388-398.

5. Johnson, W. D., P. D. Forbes, J. H. Graham, and H. R. Gray. 1966. Experimental Cutaneous Calcinosis: A Histopathologic and Histochemical Study. J. Invest. Dermatol. 43:453-466.

6. Jones, J. W. and R. T. Overman. 1948. Use and Calibration of 100% Geometry Ion Chamber. Oak Ridge National Laboratory, AECD-2367.

7. Miller, C. F. 1957. Response Curves for USNRDL 4-pi Ionization Chamber. U. S. Naval Radiological Laboratory, USNRDL-TR-155.

8. Mackin, J. L., L. W. Weisbecker, and P. E. Zigman. 1965. Radionuclide Release from Aero-Space Nuclear Reactor Fuels II. Phase One: Pulsed Neutron Irradiation of Dry Fuel. U. S. Naval Radiological Defense Laboratory, USNRDL-TR-S11, 18 January.

9. Mikhail, S. Z. 1970. Tissue Beta Radiation Doses From Particulate Fission Product Sources: Comparison of Model Predictions With Experimental and Monte Carlo Values. ESA-TR-70-01 Environmental Science Associates Technical Report.

10. Loevinger, R. 1953. Extrapolation Chamber for the Measurement of Beta Sources. Rev. Sci. Instr. 24:907.

11. Mikhail, S. Z. and K. A. Collins. 1968. Analysis of the Particulate Effluent Data From Phoebus IB.EP-IV Nuclear Reactor Test. U. S. Naval Radiological Defense Laboratory, USNRDL-TR-68-23.

12. Krebs, J. 1967. The Response of Mammalian Skin to Irradiation with Particles of Reactor Debris. U. S. Naval Radiological Defense Laboratory, USNRDL-TR-67-118.

13. Ulberg, J. D. and D. B. Kochendorfer, 1966. Models for Estimating Beta Dose to Tissue from Particle Debris in Aerospace Nuclear Applications. U. S. Naval Radiological Defense Laboratory, USNRDL-TR-1107.

14. Spencer, L. V. 1959. Energy Dissipation by Fast Electrons. National Bureau of Standards, NBS Monograph 1, 1 September.

15. Archambeau, J. O. and G. R. Mathieu. 1969. Comparison of the Observed Results of Irradiation on the Skin With Those Expected from an Idealized Model. Rad. Res. 40:285-297.

16. Snedecor, George W. 1956. Statistical Methods. The Iowa State College Press.

17. Straile, William E. and Herman B. Chase. 1963. The Use of Elongate Micro Beams of X-rays for Simulating the Effects of Cosmic Rays on Tissue: A Study of Wound Healing and Hair Follicle Regeneration. Rad. Res. 18:65-75.

18. Curtis, Howard J. 1967. The Use of a Deuteron Microbeam for Simulating the Biological Effects of Heavy Cosmic-Ray Particles. Rad. Res. 32:250-257.

19. Traenkle, Herbert L. 1962. X-ray-Induced Skin Cancer In Man. NCI Monograph 10:423.

20. Hulse, E. V. 1967. Incidence and Pathogenesis of Skin Tumors in Mice Irradiated with Single External Doses of Low Energy Beta Particles. Br. J. of Cancer:21, No. 3.

21. Albert, R. E., M. E. Phillips, P. Bennett, F. Burns and R. Heimbach. March 1969. The Morphology and Growth Characteristics of Radiation-Induced Epithelial Skin Tumors in the Rat. Cancer Research 29:658-668.

22. Schubert, G., H. A. Kunkel and G. Uhlmann. 1955. Carcinogenic Action of Different Doses of Local β-Ray Irradiation, Progress in Radiobiology, edited by Joseph S. Mitchell, Barbara E. Holmes and Cyril L. Smith. Charles C. Thomas, Springfield. pp. 480-484.

23. Rubin, Philip and George W. Casarett. 1968. Skin and Adnexa, Chapt. 3 in Clinical and Radiation Pathology. W. B. Saunders Co., Philadelphia.

24. Emery, E. W., J. Denekamp, and M. M. Ball. 1970. Survival of Mouse Skin Epithelial Cells Following Single and Divided Doses of X-rays. Rad. Res. 41:450-466.

25. Sanders, Charles L., Roy C. Thompson and W. J. Bair. 1969. Carcinogenesis in the Lung From Inhalation of Radioactive Particles. Report Contract N00228-68-1421 to USNRDL (CFSTI Document #AD690576).

Parts of this work supported by Contracts
ERDA E(11-1)-2366, SNPN-49,
USNRDL N00 228 68 C 0571 and N00 69 C 1303
And by NIH Grants ES 00269 and CA 11536